ORIGIN OF ENERGETIC ELASTICITY AND ENTROPIC ELASTICITY OF NATURAL RUBBER WITH NANODIAMOND NANOMATRIX STRUCTURE

ASANGI GANNORUWA,[1] YUANBING ZHOU,[1] KENICHIRO KOSUGI,[1] YOSHIMASA YAMAMOTO,[2] SEIICHI KAWAHARA[1,*]

[1]DEPARTMENT OF MATERIALS SCIENCE AND TECHNOLOGY, FACULTY OF ENGINEERING, NAGAOKA UNIVERSITY OF TECHNOLOGY, 1603-1 KAMITOMIOKA, NAGAOKA, NIIGATA 940-2188, JAPAN
[2]NATIONAL INSTITUTE OF TECHNOLOGY, TOKYO COLLEGE, 1220-2, KUNUGIDA, HACHIOJI, TOKYO 193-0997, JAPAN

RUBBER CHEMISTRY AND TECHNOLOGY, Vol. 94, No. 4, pp. 704–719 (2021)

ABSTRACT

The origin of energetic elasticity in conjunction with the entropic elasticity for natural rubber with a nanodiamond nanomatrix structure was investigated in terms of bound rubber formed between nanodiamonds, based on the interaction between natural rubber and nanodiamonds inside the nanomatrix. The natural rubber with a nanodiamond nanomatrix structure was prepared by reacting nanodiamonds with deproteinized natural rubber in the presence of *tert*-butylhydroperoxide/tetraethylenepentamine at 30 °C in the latex stage followed by drying. Morphology of the products was observed by two-dimensional and three-dimensional transmission electron microscopies. The effect of bound rubber on the mechanical properties of the products was investigated by measurements of the dynamic mechanical properties and differential scanning calorimetry. The contribution of bound rubber was estimated by combining the Takayanagi equation and modified Guth–Gold equation. A significant increase in complex modulus was attributed to the effect of the bound rubber. [doi:10.5254/rct.21.79923]

INTRODUCTION

Natural rubber with a nanodiamond nanomatrix structure realizes not only entropic elasticity but also energetic elasticity. This unique elasticity may be related to the chemical linkages formed between natural rubber particles and nanodiamonds, in which the nanomatrix structure retains its morphology because of chemical pinning.[1] The chemical linkages may produce bound rubbers on the surface of the nanodiamonds, which may bind nanodiamonds to each other. In fact, in previous studies, natural rubber with a nanodiamond nanomatrix structure was prepared by forming chemical linkages between natural rubber particles and nanodiamonds in the presence of a radical initiator in the latex stage. It was found that natural rubber particles with a diameter of about 1 μm were dispersed in the nanomatrix of the nanocomposite, consisting of natural rubber and nanodiamonds, in which nanodiamonds with a diameter of less than 5 nm were finely dispersed at intervals of several nanometers. The rubber present between the nanodiamonds is regarded as the bound rubber.

Bound rubber has been investigated using pulse NMR spectroscopy,[2–4] amplitude modulation atomic force microscopy,[5,6] differential scanning calorimetry (DSC),[7] and dynamic mechanical analysis (DMA),[8] among other methods. It is divided into two layers: a highly immobile, glassy hard layer (GH layer) on carbon black and a less mobile, sticky hard (SH) layer on the GH layer.[9] The thicknesses of the GH layer and SH layer were estimated to be about 10 nm, and the modulus of the bound rubber was determined to be 8.4 and 10.6 MPa.[10,11] In previous studies,[12–14] the distance between the nanodiamonds was found to be less than 10 nm. Thus, bound rubbers that are constrained in narrow spaces between nanodiamonds may be hypothesized to be harder than ordinary bound rubbers formed on the surface of carbon black. It is necessary to prove this hypothesis to understand the origins of not only the entropic elasticity but also the energetic elasticity.[15]

*Corresponding author. Email: kawahara@mst.nagaokaut.ac.jp

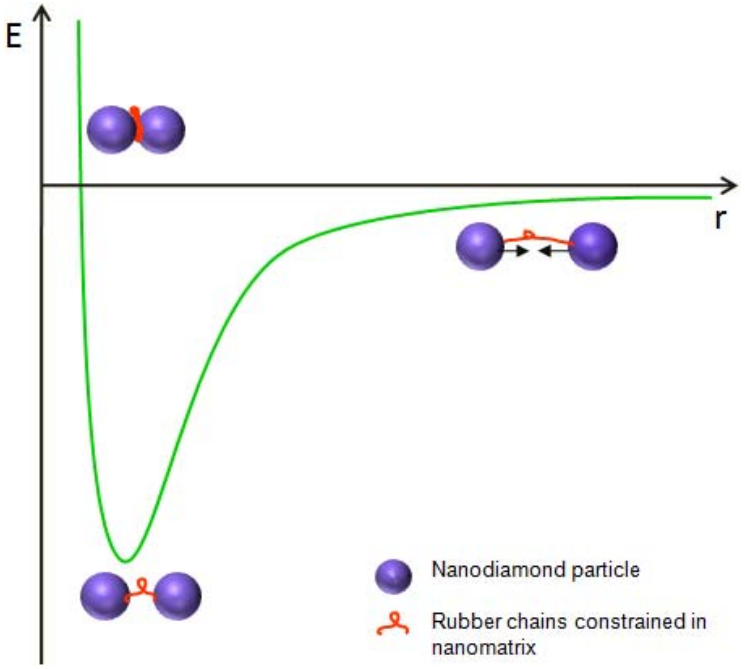

FIG. 1. — Energetic elasticity generation via bond energy.

In the present work, the bound rubbers expected to exist between the nanodiamonds in the nanomatrix were investigated using DSC and DMA. First, the modulus of the bound rubbers was estimated from the moduli of the natural rubber and natural rubber with a nanodiamond nanomatrix structure (DPNR-ND) using the equation of the Takayanagi model and Guth–Gold equation. Second, the bound rubbers were proved to exist in DPNR-ND via DSC and DMA. The generation of not only the entropic elasticity but also the energetic elasticity was related to the bound rubbers and the morphology characteristic of DPNR-ND.

BACKGROUND

The generation of not only entropic elasticity but also energetic elasticity may be attributed to the nanomatrix structure; that is, the entropic elasticity is assigned to the natural rubber particles, and the energetic elasticity is assigned to the nanomatrix of nanocomposite consisting of natural rubber and nanodiamonds. The entropic elasticity is well known to be the rubber elasticity because of the anisotropic orientation generated by the deformation of the rubber. In contrast, the energetic elasticity is the elasticity due to an increase in potential energy generated by the strain of the lattice. A plausible potential energy curve is illustrated in Figure 1, assuming that the lattice is formed with nanodiamonds. The energetic elasticity may be attributed to attractive force and repulsive force, which may occur between nanodiamonds. The attractive force may be explained to be due to a contribution of the bound rubber that binds the nanodiamonds to each other, whereas the repulsive force may be due to an excluded volume effect of the nanodiamonds, whose modulus is about 560 GPa.[16,17]

The contribution of the bound rubber may be explained to be due to the effect of the bridged filler network, which is formed with nanodiamonds, according to Figure 2. The bridged filler network may be formed by the reaction of a rubber molecule with two nanodiamonds or more,

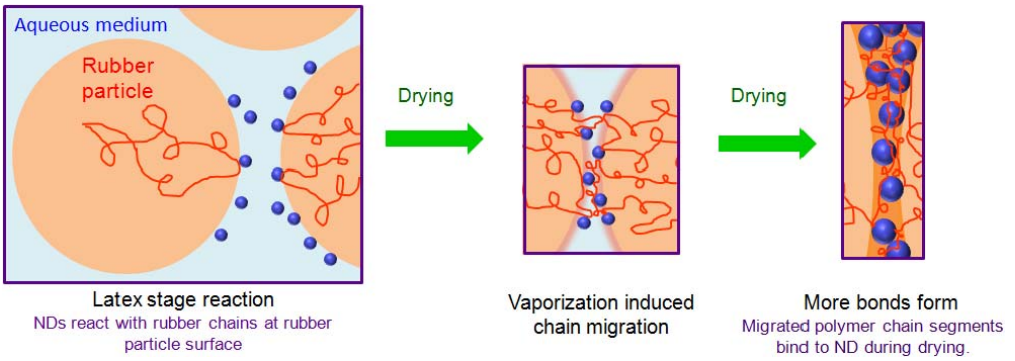

FIG. 2. — Rubber chains constrained between nanodiamond particles inside the nanomatrix structure.

according to the literature.[15] In the case of natural rubber with a nanodiamond nanomatrix structure, the chemical linkages between the natural rubber molecule of the rubber particle and nanodiamonds are formed with a radical initiator in the latex stage, after deproteinization.[18–20] The resulting rubber molecule linking to nanodiamonds is required to react with the other nanodiamonds linking to the natural rubber molecule of the other rubber particle during drying. Hence, the space between the nanodiamonds may be filled with natural rubber to form the bound rubber as a bridged filler network, as illustrated in Figure 3. In this case, the modulus of the natural rubber as a bound rubber is expected to be higher than that of ordinary natural rubber.[21]

EXPERIMENTAL

MATERIALS

Deproteinized natural rubber (DPNR) was prepared by incubating high-ammonia natural rubber latex at a dry rubber content (DRC) of 30 w/w% (DRC 62.6 w/w%; Golden Hope, Kuala Lumpur, Malaysia) dispersed in 0.1 w/w% sodium dodecyl sulfate (99%; Kishida Chemical, Osaka, Japan) with 0.1 w/w% $CO(NH_2)_2$ (99%; Nacalai Tesque, Kyoto, Japan) at room temperature.[22] The nanodiamond slurry was prepared by dispersing nanodiamond solid (<10 nm;

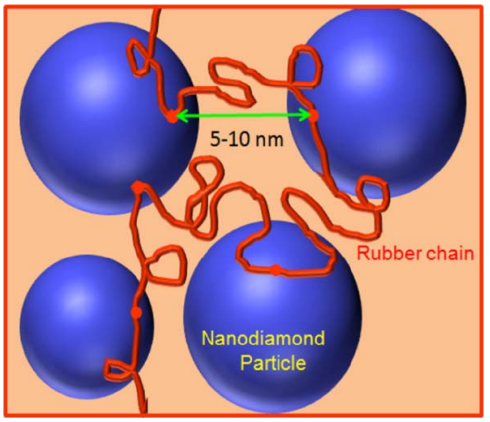

FIG. 3. — Schematic representation of a rubber chain bound to nanodiamond particles at multiple points inside the nanomatrix.

Sumiseki Materials, Tokyo, Japan) in conc. ammonia (18 g, 28%; Nacalai Tesque) and homogenized for 60 min (Usonic U-D6354 ultrasonic generator at 21 kHz; Cho-onpa Kogyo, Tokyo, Japan). The mixture of nanodiamond slurry and DPNR latex (DRC = 30 w/w%) was charged with N_2(g) for 1 h at 30 °C. The mixture then reacted in the presence of *tert*-butylhydroperoxide (TBHP; 68%; Kishida Chemical) and tetraethylenepentamine (TEPA; 95%; Kishida Chemical) for 4 h in an N_2-saturated environment. The DPNR-ND latex was cast onto a glass Petri dish to prepare the 1 mm thick films. To study the effect of initiator, a 25 w/w% nanodiamond concentration was used, as it is in the critical concentration region for the nanomatrix formation.

MECHANICAL PROPERTIES

The dynamic viscoelasticity was measured using an Anton Paar Physica MCR 301 with parallel plate geometry (12 mm diameter) at an angular frequency ranging starting at 0.1 rad s^{-1}. The measurements were performed at 25 °C in the linear viscoelasticity region. To obtain the vertical shift factor, viscoelastic measurements were performed in an angular frequency range from 0.1 to 100 rad s^{-1}. The measurements were performed between –70 and 130 °C in the linear viscoelasticity region.

BOUND RUBBER CONTENT

The insoluble rubber fraction (i.e., bound rubber content) for DPNR-ND was determined by Wolf's method based on the swelling technique. The DPNR-ND was cut into tiny pieces and immersed in toluene for 7 days. By centrifugation of the mixture at 10,000*g*, the insoluble rubber fraction (gel) was separated from soluble (sol) fraction. The gel fraction was dried at 50 °C until a constant weight was attained. The bound rubber content, BR (w/w%), was estimated as follows[23]:

$$\mathrm{BR(w/w\%)} = \frac{W_g - (W_i \times m_f)}{W_i \times m_r} \times 100 - \mathrm{BR_0} \quad (1)$$

where BR_0 is the gel content of the DPNR, W_g is the weight of the filler and the gel fraction, W_i is the initial weight of the sample, and m_f and m_r are the weight fractions of the filler and rubber used to prepare the samples, respectively.

MORPHOLOGY

Distribution of the nanoparticles and the nanodiamond particle size was observed by two-dimensional (2D) and three-dimensional (3D) transmission electron microscopy (TEM) by JEOL JEM-2100 at an accelerating voltage of 200 kV. Ultra-thin sections for the TEM observations were prepared by Richer-Nissei FC-S Ultracut microtome at –90 °C under N_2. Ultra-thin sections were placed on Cu grids for the TEM observation. For 3D TEM measurements, a series of 2D TEM images were obtained by tilting the samples from –60° to +60° with 1° increments at 15,000× magnifications. The alignment and reconstruction of the 3D TEM images were performed according to a previously described protocol.[24]

DIFFERENTIAL SCANNING CALORIMETRY

The DSC measurements were performed using an SII nanotechnology EXSTAR DSC 7020 analyzer from –150 to 150 °C at a definite heating rate of 10 °C/min using an Al pan.

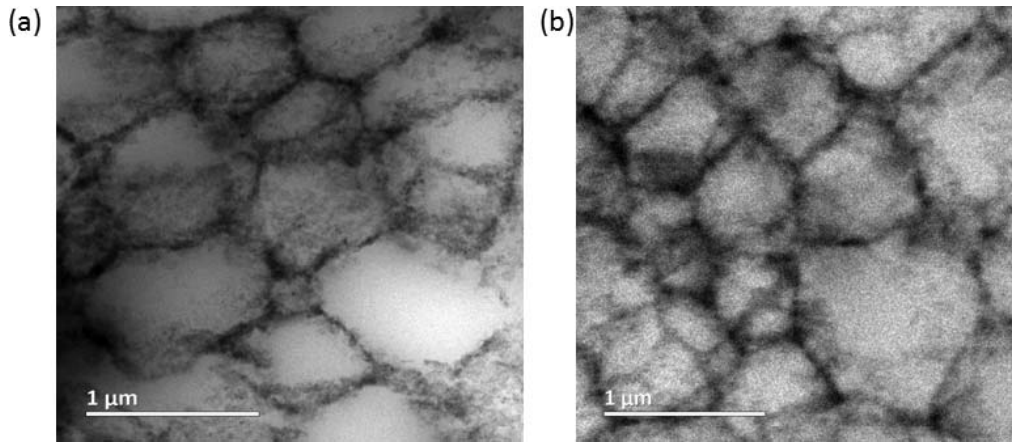

FIG. 4. — TEM images of the nanodiamond nanomatrix structure containing 25 w/w% ND concentration and (a) 6.6×10^{-5} mol/g-rubber TBHP/TEPA and (b) 3.3×10^{-4} mol/g-rubber TBHP/TEPA.

The bound rubbers for the DSC analysis were obtained by immersing DPNR-ND cut into small pieces into dry toluene for 5 days under dark. The insoluble gel fraction was recovered from the toluene solution after centrifugation at 10,000*g*. The gel fraction was dried at 50 °C until a constant weight was obtained.

RESULTS AND DISCUSSION

Figure 4 shows TEM images for DPNR-NDs with 25 w/w% nanodiamond, prepared with 6.6×10^{-5} mol/g-rubber TBHP/TEPA and 3.3×10^{-4} mol/g-rubber TBHP/TEPA, respectively. The bright domains represent natural rubber, and the dark domains represent nanodiamonds. Natural rubber particles with a diameter of about 1 μm were dispersed in the nanodiamond nanomatrix with a thickness of a few tens of nanometers, in which nanodiamonds were closely packed in the nanomatrix. The diameter of the natural rubber particles and the thickness of the nanomatrix for DPNR-ND prepared with 25 w/w% nanodiamond and 6.6×10^{-5} mol/g-rubber TBHP/TEPA were similar to those for DPNR-ND prepared with 25 w/w% nanodiamond and 3.3×10^{-4} mol/g-rubber TBHP/TEPA. Thus, the nanomatrix structure was found to be independent of the TBHP/TEPA concentration. This may be explained to be due to the same nanodiamond concentration. The dispersion of nanodiamonds in the nanomatrix was investigated, in detail, through 3D TEM observation. The 3D TEM images for DPNR-ND are given in Figure 5, in which the white domains represent the nanodiamonds. In the 3D TEM images, nanodiamonds with a diameter of less than 10 nm were dispersed uniformly in the nanomatrix. The distance between nanodiamonds was about 7 nm in average. The diameter of the nanodiamonds and their dispersity for DPNR-ND prepared with 25 w/w% nanodiamond and 6.6×10^{-5} mol/g-rubber TBHP/TEPA were similar to those for DPNR-ND prepared with 25 w/w% nanodiamond and 3.3×10^{-4} mol/g-rubber TBHP/TEPA. In previous studies,[12–14] the values of the stress at break for DPNR-NDs were found to be higher than that of neat DPNR, suggesting that the space between nanodiamonds was filled with natural rubber. The filled rubber may be considered to be less mobile than neat DPNR.[3,4,9]

Figure 6a,b shows the plot of gel content and bound rubber content of DPNR-NDs versus nanodiamond concentration at a constant initiator concentration and the plot of gel content and bound rubber content versus initiator concentration at a definite nanodiamond concentration (25 w/w%), respectively. In Figure 6a, both the gel content and the bound rubber content of DPNR-ND

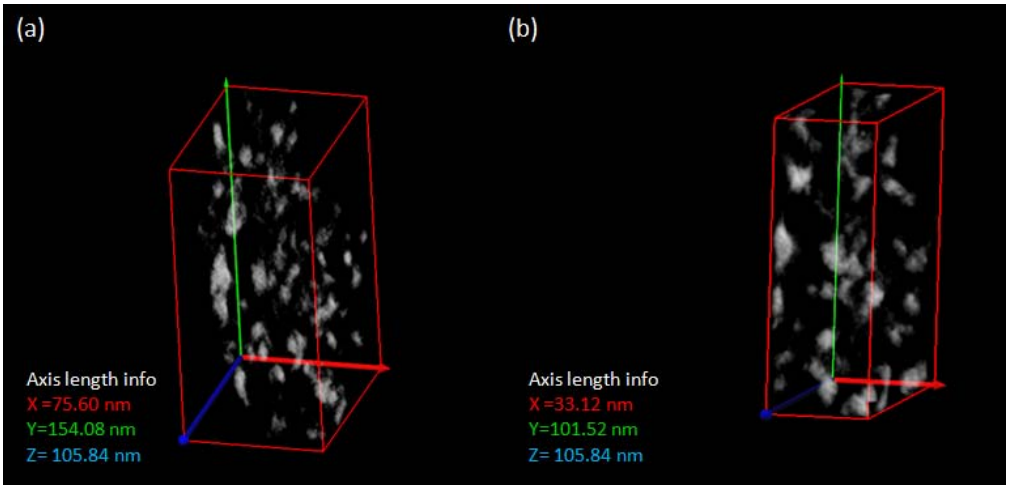

FIG. 5. — Three-dimensional TEM image of nanodiamond nanomatrix containing 25 w/w% nanodiamond concentration prepared with (a) 3.3×10^{-4} mol/g-rubber TBHP/TEPA and (b) 6.6×10^{-5} mol/g-rubber TBHP/TEPA.

prepared with 6.6×10^{-5} mol/g-rubber TBHP/TEPA increased as the nanodiamond concentration increased. For instance, the gel content was 91.9 w/w% for DPNR-ND containing 40 w/w% nanodiamond, whereas it was 37.7 w/w% for neat DPNR. On the contrary, in Figure 6b, the gel content gradually increased as the initiator concentration increased at the nanodiamond concentration of 25 w/w%, whereas the bound rubber content significantly increased. For instance, the bound rubber contents of DPNR-NDs prepared with TBHP/TEPA of 6.6×10^{-5} mol/g-rubber and 3.3×10^{-4} mol/g-rubber were 28.3 and 39.7 w/w%, respectively. These values imply that the number of chemical linkages between natural rubber and nanodiamonds is dependent on not only the nanodiamond concentration but also the initiator concentration; the higher the nanodiamond concentration and the initiator concentration, the larger the number of chemical linkages.

Figure 7 shows DSC thermograms for DPNR-NDs prepared with 25 w/w% nanodiamond and various amount of TBHP/TEPA. The thermograms showed a sudden drop in heat capacity at –67 °C, suggesting that a glass transition occurred. The glass transition temperature (T_g) was thus determined to be an inflection point of the DSC thermogram. The T_g values were the same as each other; that is, the T_g was independent of TBHP/TEPA concentration. In addition, in the DSC thermograms, a minor drop occurred at 41 °C. The minor drop may be attributed to some transition of natural rubber, because only both natural rubber and nanodiamond have been used to prepare DPNR-ND. This may be explained to be due to the constrained natural rubber (Figure 2), as reported in the literature.[25] Thus, the minor drop in heat capacity was attributed to the glass transition temperature of the constrained natural rubber present in the nanomatrix, that is, the bound rubbers.

Figure 8 shows complex modulus of DPNR-ND versus the strain amplitude. Complex modulus of DPNR was independent of strain amplitude, whose value was 0.2 MPa. The Payne effect was clearly observed for DPNR-ND prepared with 3.3×10^{-4} mol/g-rubber of TBHP/TEPA in Figure 8a; that is, complex modulus decreased with increasing strain amplitude. This may be attributed to the scission of chemical linkages between natural rubber and nanodiamonds, because the higher the initiator concentration, the larger the number of chemical linkages, as shown in Figure 6b. The Payne effect was also observed for DPNR-ND prepared with 30 and 40 w/w% of nanodiamond, whereas complex moduli of those prepared with 10 and 20 w/w% of nanodiamond were independent of strain amplitude, as shown in Figure 8b. The bound rubber content of DPNR-

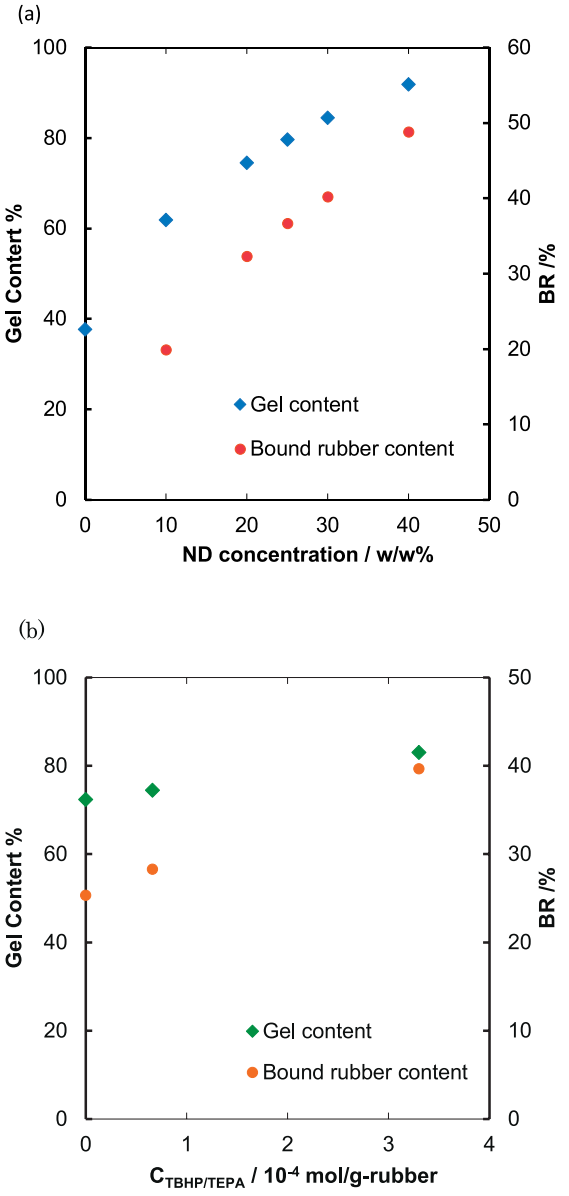

FIG. 6. — Gel content and bound rubber content with respect to (a) nanodiamond concentration at 6.6×10^{-5} mol/g-rubber TBHP/TEPA concentration and (b) TBHP/TEPA initiator concentration at 25 w/w% nanodiamond concentration.

ND increased as the nanodiamond concentration increased, as shown in Figure 6a. Therefore, the Payne effect of DPNR-ND at a higher nanodiamond concentration might be explained as being due to not only the filler–filler interaction but also the scission of chemical linkages between natural rubber and nanodiamond.

Figure 9 shows the temperature dependence of the storage modulus (G'), loss modulus (G''), and loss tangent (tanδ) of DPNR-ND prepared with 25 w/w% nanodiamonds and various amounts of TBHP/TEPA. The G', G'', and tanδ were dependent on temperature. For instance, a sudden drop in G' appeared at –65 °C, whereas peaks in the G'' and tanδ appeared at –65 °C and –62.5 °C,

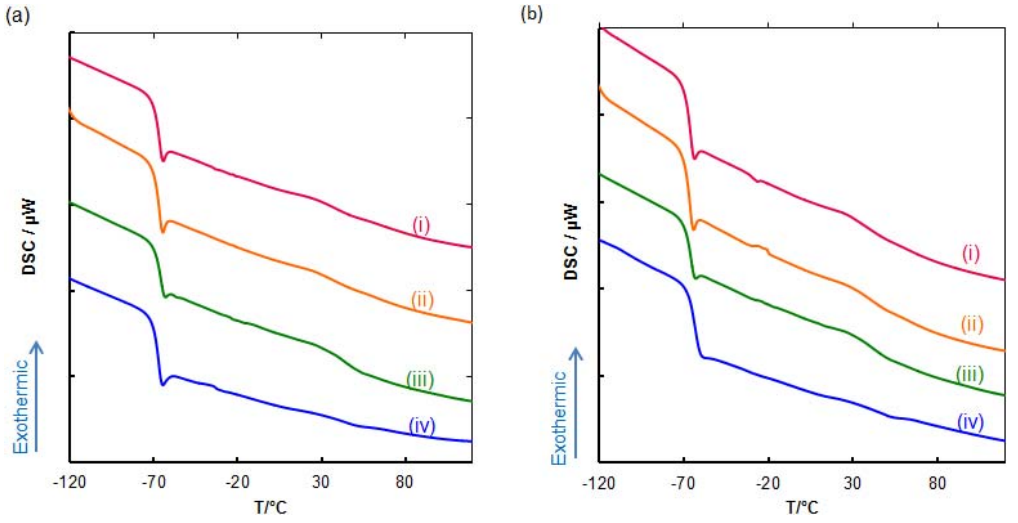

FIG. 7. — DSC curves of (a) DPNR-ND and (b) bound rubber fraction of DPNR-ND extracted by toluene containing 25 w/w% nanodiamond concentration prepared with (i) 3.3×10^{-4} mol/g-rubber, (ii) 6.6×10^{-5} mol/g-rubber, TBHP/TEPA initiator (iii) without initiator and (iv) neat DPNR.

respectively. These were attributed to the glass transition of the natural rubber. The glass transition (T_g) was determined as a peak top of tanδ (i.e., –62.5 °C). Above T_g, a rubbery plateau region appeared. In the rubbery plateau region, values of G' and G'' smoothly varied. In contrast, in the tanδ for DPNR-ND prepared with TBHP/TEPA, a small peak appeared at 40 °C. The peak at 40 °C may correspond to the minor drop in DSC thermogram at 41 °C. Thus, the small peak at 40 °C was attributed to the T_g of the constrained natural rubber present in the nanomatrix.

Figure 10 shows a plot of complex modulus at 25 °C and 1 rad/s versus volume fraction of nanodiamond for DPNR-ND prepared with 6.6×10^{-5} mol/g-rubber TBHP/TEPA and DPNR-ND prepared without TBHP/TEPA. The value of complex modulus of DPNR-ND increased as the volume fraction of nanodiamond increased, in which the value of complex modulus of DPNR was 1.49×10^5 Pa, as reported in the literature.[26,27] The values of complex modulus of DPNR-ND prepared with 6.6×10^{-5} mol/g-rubber TBHP/TEPA were larger than values estimated by the

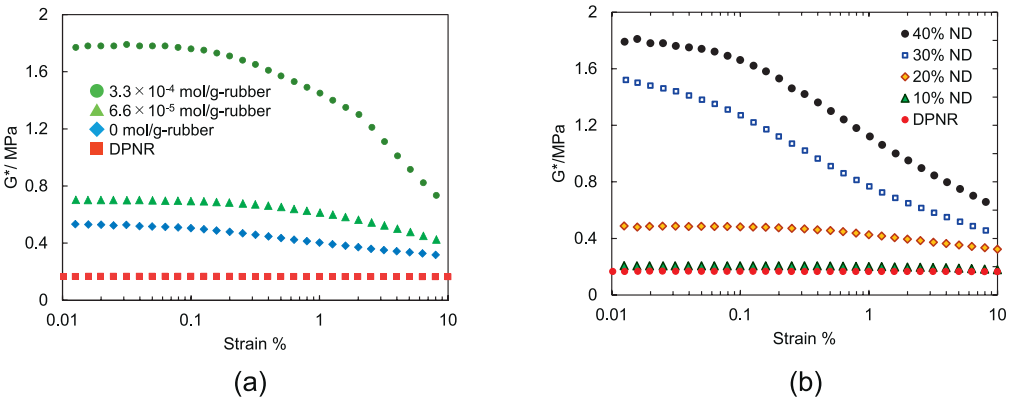

FIG. 8. — Complex modulus of DPNR-ND vs the strain amplitude, (a) effect of the amount of radical initiator, (b) effect of the amount of ND.

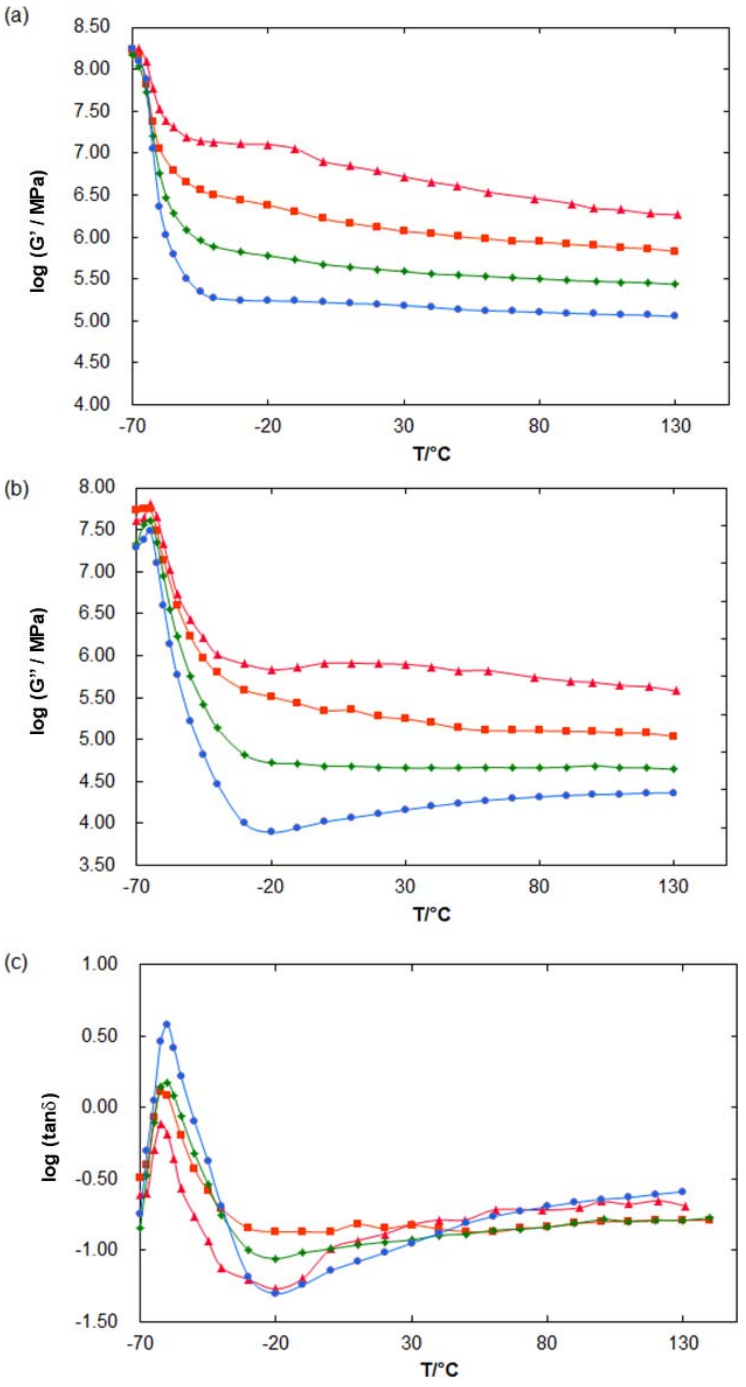

FIG. 9. — Temperature dependency of (a) storage modulus (G'), (b) loss modulus (G''), and loss tangent (tanδ) of DPNR-ND containing 25 w/w% nanodiamond concentration prepared with (▲) 3.3×10^{-4} mol/g-rubber, (■) 6.6×10^{-5} mol/g-rubber, TBHP/TEPA initiator (◆) without initiator, and (●) neat DPNR measured at 1 rad s^{-1} angular frequency in the linear viscoelasticity region.

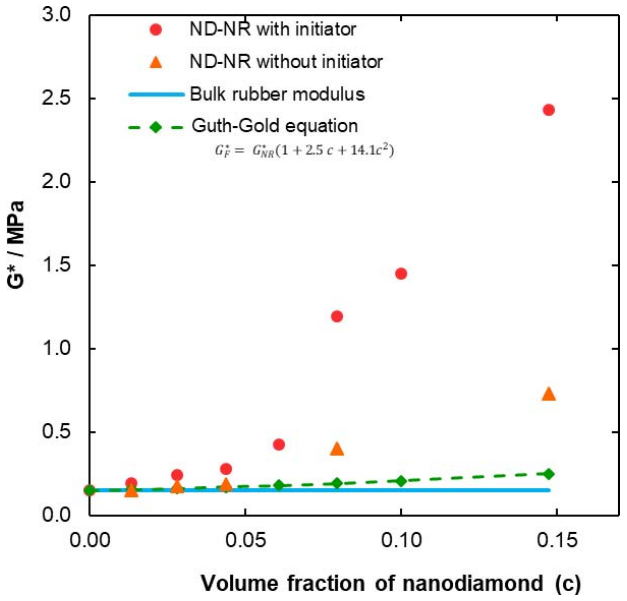

FIG. 10. — Complex modulus (G^*) of DPNR-ND prepared (●) with and (▲) without TBHP/TEPA initiator, (◆) calculated from the Guth–Gold equation, and (—) bulk rubber measured at 25 °C, 1 rad s^{-1} angular velocity in the linear viscoelasticity region.

Guth–Gold equation in all investigated volume fraction regions; in particular, the difference between the values of complex modulus and the estimated values was more significant at a volume fraction of 0.05 or more. In contrast, the values of complex modulus of DPNR-ND prepared without TBHP/TEPA were in good agreement with the values estimated by the Guth–Gold equation at a volume fraction of 0.05 or less, whereas they were significantly distinguished from the estimated values at a volume fraction of 0.05 or greater. The difference between the values of complex modulus and the estimated values may be attributed to the formation of the nanomatrix structure, as in the case of the filler network structure.[28]

Figure 11 shows a plot of complex modulus at 25 °C and 1 rad/s versus the TBHP/TEPA concentration for DPNR-ND prepared with 25 w/w% nanodiamonds and 15 w/w% nanodiamonds. The nanomatrix structure was formed for DPNR-ND prepared with 25 w/w% nanodiamonds but not for DPNR-ND prepared with 15 w/w% nanodiamonds. For DPNR-ND prepared with 25 w/w% nanodiamonds and DPNR-ND prepared with 15 w/w% nanodiamonds, the value of complex modulus for DPNR-ND increased as the initiator concentration increased. For instance, the values of complex moduli of DPNR-ND containing 25 w/w% nanodiamond prepared with TBHP/TEPA of 6.6×10^{-5} mol/g-rubber and 3.3×10^{-4} mol/g-rubber were 1.19 and 5.79 MPa, respectively, which are about 8 times and 38 times higher than the value of complex modulus of neat DPNR. These imply that the modulus of DPNR-ND is dependent on the number of chemical linkages between natural rubber and nanodiamonds. Hence, the increase in the value of complex modulus of DPNR-ND may be attributed to the amount of the bound rubbers generated by forming chemical linkages between natural rubber and nanodiamonds.

The nanomatrix structure is schematically illustrated in Figure 12a. The nanomatrix structure may be divided into two domains: the neat rubber domain and the nanocomposite domain consisting of rubber and nanodiamonds. The neat rubber domain and the nanocomposite domain may be combined to make series and parallel models, as shown in Figure 12b. Using the series and

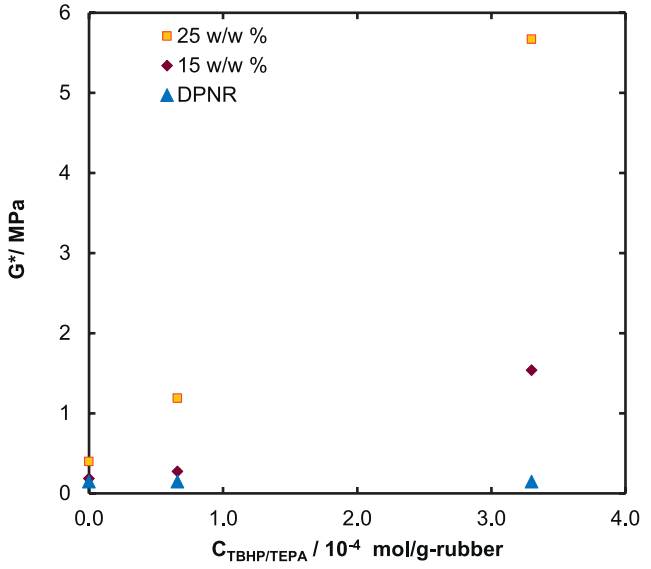

FIG. 11. — Complex modulus (G^*) of DPNR-ND at 25 and 15 w/w% nanodiamond concentration with respect to initiator concentration measured at 25 °C, 1 rad s^{-1} angular velocity in the linear viscoelasticity region.

parallel models (i.e., the Takayanagi model[29–31]), complex modulus (G^*) of the DPNR-ND is expressed by the following equation:

$$\frac{1}{G^*} = \frac{\varphi}{\lambda G^*_{\mathrm{NR}} + (1-\lambda) G^*_{\mathrm{NM}}} + \frac{(1-\varphi)}{G^*_{NM}} \tag{2}$$

where λ and φ represent the volume fractions of the fragments in series and parallel models, respectively, and G^*_{NR} is the modulus of the neat rubber and G^*_{NM} is the modulus of the nanomatrix structure. The volume fraction of the natural rubber (V_{NR}) as a neat rubber is related to λ and φ, as shown in Eqs. 3 and 4.[30,31]

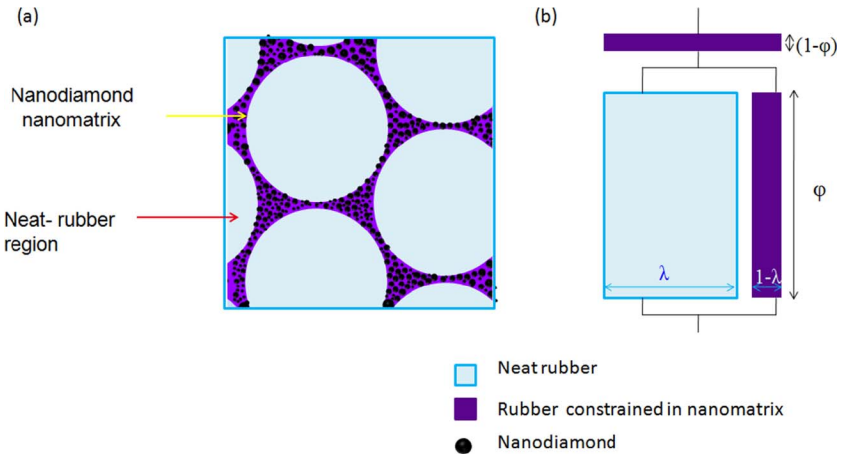

FIG. 12. — (a) Schematic representation of the nanodiamond nanomatrix structure. (b) Series and parallel model developed based on the Takayanagi model.

$$\lambda = \frac{(2 + 3V_{NR})}{5} \tag{3}$$

$$\varphi = \frac{5V_{NR}}{(2 + 3V_{NR})} \tag{4}$$

The modulus of the nanocomposite as a nanomatrix is expressed by the Guth–Gold equation (Eq. 5)[26]:

$$G^*_{NM} = G^*_{gum}(1 + 2.5c + 14.1c^2) \tag{5}$$

where c is the volume fraction of the filler and G^*_{NM} and G^*_{gum} are the moduli of the nanomatrix structure and gum, respectively. The value of G^*_{NM} is expected to be larger than that of neat natural rubber (10^5 Pa),[29] as the value of complex modulus of DPNR-ND prepared with 6.6×10^{-5} mol/g-rubber TBHP/TEPA is about 10 times larger than that of neat rubber.

It is important to estimate the volume fraction of the nanodiamond nanomatrix (c) from the volume fraction of the nanodiamond of DPNR-ND (x).

$$c = \frac{x}{x + y(1 - x)} \tag{6}$$

$$\lambda\varphi = V_{NR} = \frac{(1 - x)(1 - y)}{x + y(1 - x) + (1 - x)(1 - y)} \tag{7}$$

$$\varphi = \frac{(1 - x)(1 - y)}{\lambda} \tag{8}$$

where y is the volume fraction of the constrained natural rubber (VBR) and is estimated as a ratio of volume of the constrained natural rubber to the volume of total natural rubber. The values of x and y were estimated from the thickness of the nanomatrix determined by TEM observation. Figure 13 shows the TEM images for the DPNR-ND prepared with various amounts of nanodiamond and TBHP/TEPA. The thickness of the nanomatrix was 100, 70, and 50 nm for DPNR-NDs prepared with 40, 30, and 25 w/w% nanodiamonds in the presence of 6.6×10^{-5} mol/g-rubber TBHP/TEPA, respectively. In contrast, for DPNR-ND prepared with 25 w/w% nanodiamonds and 3.3×10^{-4} mol/g-rubber TBHP/TEPA, the thickness of the nanomatrix was 50 nm. The volume fractions of the natural rubber (V_{NR}) and nanomatrix (V_{NM}) were estimated from the diameter of the natural rubber particles and the thickness of the nanomatrix by the following equations, assuming that the rubber particles covered with the nanomatrix were right spheres, as shown in Figure 14. Estimated values of V_{NR} and V_{NM} are shown in Table I. The values of V_{NR} and V_{NM} of DPNR-ND prepared with 25 w/w% nanodiamonds and 6.6×10^{-5} mol/g-rubber TBHP/TEPA were the same as those of DPNR-ND prepared with 25 w/w% nanodiamonds and 3.3×10^{-4} mol/g-rubber TBHP/TEPA.

$$V_{NR} = \frac{{}^4\!/_3\pi r^3}{{}^4\!/_3\pi\left(r + \frac{T}{2}\right)^3} \tag{9}$$

$$V_{NM} = \frac{{}^4\!/_3\pi\left(r + \frac{T}{2}\right)^3 - {}^4\!/_3\pi r^3}{{}^4\!/_3\pi\left(r + \frac{T}{2}\right)^3} \tag{10}$$

The G^*_{NM} and G^*_{gum} were estimated from G^*, G^*_{NR}, V_{NR}, and V_{NM}. The estimated values of G^*_{NM} and G^*_{gum} are shown in Table II. The value of G^*_{NM}, estimated by Eq. 2, increased from 12 to 14 MPa,

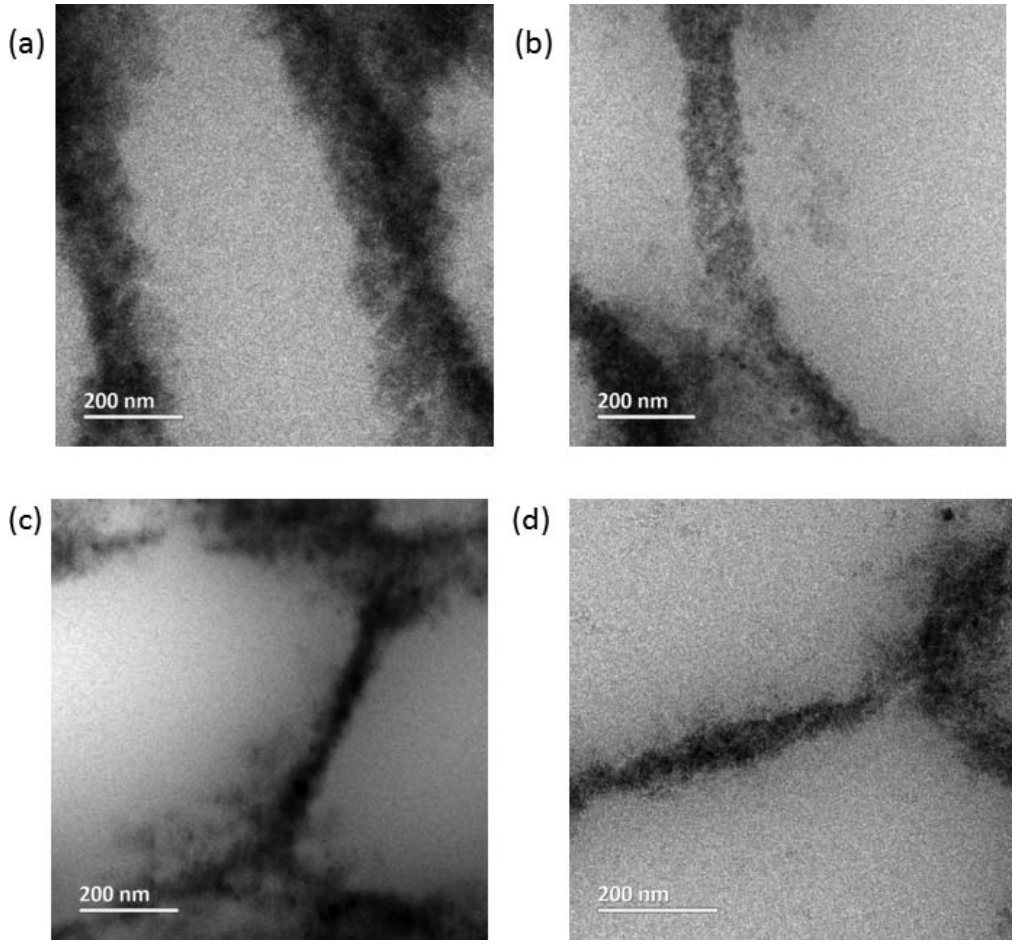

FIG. 13. — TEM images of DPNR-ND prepared with 6.6×10^{-5} mol/g-rubber TBHP/TEPA and (a) 40 w/w%, (b) 30 w/w %, (c) 25 w/w% nanodiamonds and (d) 25 w/w% nanodiamonds 3.3×10^{-4} mol/g-rubber TBHP/TEPA.

as the nanodiamond concentration increased. Similarly, the value of G^*_{gum} increased from 1.6 to 1.8 MPa, since the G^*_{gum} was estimated from G^*_{NM}. The value of G^*_{gum} of prepared DPNR-ND was similar as that reported in the literature.[10,11] In addition, the volume fraction of the bound rubbers increased from 0.06 to 0.12 as the nanodiamond concentration increased. Consequently, the

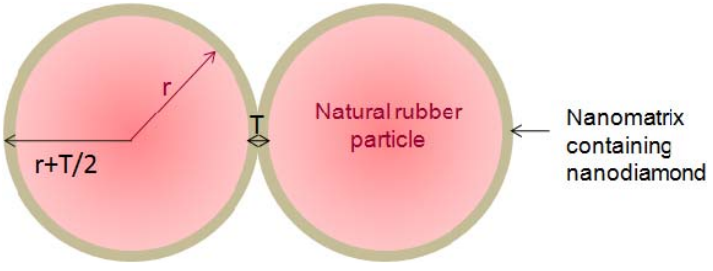

FIG. 14. — (a) Schematic representation of the nanodiamond nanomatrix structure in which the rubber particle of the radius is surrounded by nanomatrix of thickness *T*.

TABLE I
ESTIMATED VOLUME FRACTION OF NANOMATRIX AND NEAT RUBBER BY 2D TEM (FIGURE 12) DPNR-ND PREPARED WITH[a]

No.	Label, w/w% ND	T_{NM}, nm	V_{NM}	V_{NR}	x	y
6.6×10^{-5} mol/g-rubber TBHP/TEPA						
1	25	50	0.136	0.864	0.08	0.061
2	30	70	0.184	0.816	0.10	0.093
3	40	100	0.249	0.751	0.15	0.116
3.3×10^{-4} mol/g-rubber TBHP/TEPA						
4	25	50	0.137	0.863	0.08	0.062

[a] V_{NR}, volume fraction of neat rubber; V_{NM}, volume fraction of nanomatrix structure; T_{NM} , thickness of the nanomatrix structure.

modulus and the volume fraction of the bound rubbers were found to be dependent on the nanodiamond concentration.

Table II also shows the G^*_{gum} for DPNR-ND prepared with 25 w/w% nanodiamonds and 3.3×10^{-4} mol/g-rubber TBHP/TEPA. The value of G^*_{gum} was 8.73 MPa, which was about 5 times larger than the modulus of DPNR-ND prepared with 25 w/w% nanodiamonds and 6.6×10^{-5} mol/g-rubber TBHP/TEPA. The increase in the modulus of the bound rubbers may be explained to be due to the increase in chemical linkages between natural rubber and nanodiamonds (Figures 2 and 3), since the value of V_{BR} of DPNR-ND prepared with 25 w/w% nanodiamonds and 3.3×10^{-4} mol/g-rubber TBHP/TEPA was the same as that of DPNR-ND prepared with 25 w/w% nanodiamonds and 6.6×10^{-5} mol/g-rubber TBHP/TEPA. This may be associated with the energetic elasticity of DPNR-ND, which arises from the formation of the chemical linkages between natural rubber and nanodiamonds.

TABLE II
ESTIMATED MODULUS OF THE NANOMATRIX STRUCTURE, MODULUS OF THE BOUND RUBBERS IN THE NANOMATRIX, VOLUME FRACTIONS, AND PARAMETERS OF THE TAKAYANAGI MODEL FOR DPNR-ND[a]

	Label, w/w% ND	c_{ND} (x)	V_{TNR} ($1-x$)	G^*, MPa	V_{NR}	V_{NM}	V_{BR} (y)	λ	φ	G^*_{gum}, MPa	G^*_{NM}, MPa
DPNR-ND prepared with 6.6×10^{-5} mol/g-rubber TBHP/TEPA initiator concentration											
1	40	0.15	0.85	2.43	0.751	0.249	0.116	0.8508	0.8831	1.80	13.748
2	30	0.10	0.90	1.45	0.816	0.184	0.093	0.8898	0.9174	1.67	10.921
3	25	0.08	0.92	1.19	0.864	0.136	0.061	0.9183	0.9407	1.64	12.037
DPNR-ND prepared with 3.3×10^{-4} mol/g-rubber TBHP/TEPA initiator concentration											
4	25	0.08	0.92	5.67	0.863	0.137	0.062	0.9178	0.9403	8.73	63.420

[a] c_{ND}, volume fraction of nanodiamond with total rubber; V_{TNR}, volume fraction of total rubber; G^*, experimental modulus of DPNR-ND; T_{NM}, thickness of the nanomatrix estimated by TEM images; V_{NR}, volume fraction of neat rubber; V_{NM}, volume fraction of nanomatrix structure; V_{BR}, volume fraction of the rubber inside the nanomatrix from total rubber; λ and φ represent volume fractions of the fragments in series and parallel models, respectively; G_{NM}, estimated modulus of the nanomatrix structure; G_{gum}, estimated modulus of gum inside the nanomatrix structure by the Guth–Gold equation.

CONCLUSION

Natural rubber with a nanodiamond nanomatrix structure was prepared with the TBHP/TEPA initiator in the latex stage. The nanomatrix structure was found to consist of natural rubber particles of 1 μm in average diameter dispersed in the nanodiamond nanomatrix with a thickness of few tens of nanometers, in which nanodiamonds of less than 10 nm in diameter were closely packed in the nanomatrix. The bound rubbers present in the nanomatrix were detected by DSC and DMA. The values of moduli of the nanomatrix and the bound rubber for DPNR-ND prepared with 40 w/w% nanodiamonds and 6.6×10^{-5} mol/g-rubber TBHP/TEPA were estimated to be 13 and 1.8 MPa, respectively. These values increased to 63 and 8.73 MPa for DPNR-ND prepared with 25 w/w% nanodiamonds and 3.3×10^{-4} mol/g-rubber TBHP/TEPA. The increase in the modulus of the bound rubbers was found to be due to the chemical linkages present between natural rubber and nanodiamonds. It was proved that the nanomatrix structure generated the energetic elasticity in conjunction with the entropic elasticity.

ACKNOWLEDGEMENT

This work was supported in part by a Grant-in-Aid (21K18316) for Challenging Research (Pioneering) from the Japan Society for the Promotion of Science, JST-aXis (JPMJAS2002) from the Japan Science and Technology Agency (JST), and MEXT Project (JPMXS0430300121) for promoting public utilization of advanced research infrastructure (Program for the SHARE, GIGAKU-Innovation Equipment Sharing Network) at Nagaoka University of Technology.

REFERENCES

[1]S. Kawahara, T. Kawazura, T. Sawada, and Y. Isono, *Polymer* **44**, 4527 (2003).

[2]J. O'Brien, E. Cashell, G. E. Wardell, and V. J. McBrierty, *Macromolecules* **9**, 653 (1976).

[3]T. Nishi, *J. Polym. Sci. Part B: Polym. Phys*. **12**, 685 (1974).

[4]S. Kaufman, W. P. Slichter, and D. D. Davis, *J. Polym. Sci. Part A-2: Polym. Phys*. **9**, 829 (1971).

[5]T. Igarashi, S. Fujinami, T. Nishi, N. Asao, and K. Nakajima *Macromolecules* **46**, 1916 (2013).

[6]D. Wang, S. Fujinami, H. Liu, K. Nakajima, and T. Nishi, *Macromolecules* **43**, 5521 (2010).

[7]J. C. Kenny, V. J. McBrierty, Z. Rigbi, and D. C. Douglass, *Macromolecules* **24**, 436 (1991).

[8]B. Jiang, L. Zhu, C. Zhao, and Z. Chen, *Polym. Compos*. **38**, 1112 (2015).

[9]Y. Fukahori, *J. Appl. Polym. Sci*. **95**, 60 (2005).

[10]D. Wang, S. Fujinami, K. Nakajima, K. Niihara, S. Inukai, H. Ueki, A. Magario, T. Noguchi, M. Endo, and T. Nishi, *Carbon* **48**, 3708 (2010).

[11]K. Nakajima, M. Ito, H. K. Nguyen, and X. Liang, RUBBER CHEM. TECHNOL. **90**, 272 (2017).

[12]A. Gannoruwa, M. Sumita, and S. Kawahara, *Polymer* **126**, 40 (2017).

[13]A. Gannoruwa and S. Kawahara, *Langmuir* **34**, 6861 (2018).

[14]S. Kawahara, A. Gannoruwa, K. Nakajima, L. Xiaobin, I. Akiba, and Y. Yamamoto, *Adv. Funct. Mater*. **30**, 1909791 (2020).

[15]Y. Isono and T. Aoyama, *Nihon Reoroji Gakkaishi* **41**, 137 (2013).

[16]M. Popov, V. Churkin, A. Kirichenko, V. Denisov, D. Ovsyannikov, B. Kulnitskiy, I. Perezhogin, V. Aksenenkov, and V. Blank, *Nanoscale Res. Lett*. **12**, 561 (2017).

[17]M. A. Lodes, F. S. Kachold, and S. M. Rosiwal, *Philos. Trans. R. Soc. A* **373**, 20140136 (2015).

[18]Y. Fukushima, S. Kawahara, and Y. Tanaka, *J. Rubber Res*. **1**, 154 (1998).

[19]K. Nawamawat, J. T. Sakdapipanich, C. C. Ho, J. S. Yujie Mad and J. G. Vancso, *Colloids Surf. A* **390**, 157 (2011).

[20]N. Pukkate, T. Horimai, O. Wakisaka, Y. Yamamoto, and S. Kawahara, *J. Polym. Sci. A Polym. Chem*. **47**, 4111 (2009).

[21]D. Braun, H. Cherdron, M. Rehahn, H. Ritter, and B. Voit, *Polymer Synthesis: Theory and Practice - Fundamentals, Methods, Experiments*, 5th ed., Springer, Berlin, 2013.

[22]N. H. Yusof, Y. Yamamoto, O. Yamamoto, and S. Kawahara, *Kaut Gummi Kunst* **68**, 46 (2015).

[23]S. Wolff, M.-J. Wang, and E.-H. Tan, RUBBER CHEM. TECHNOL. **66**, 163 (1993).

[24]H. Jinnai, Y. Nishikawa, T. Ikehara, and T. Nishi, "Emerging Technologies for the 3D Analysis of Polymer Structures," in *NMR • 3D Analysis • Photopolymerization. Advances in Polymer Science*, Vol. 170, Springer, Berlin, 2004.

[25]J. Berriot, H. Montes, F. Lequeux, D. Long, and P. Sotta, *Macromolecule* **35**, 9756 (2002).

[26]K. Nawamawat, J. T. Sakdapipanich, and C. C. Ho, *Macromol. Symp*. **288**, 95 (2010).

[27]N. H. Yusof, K. Noguchi, L. Fukuhara, Y. Yamamoto, and S. Kawahara, *Colloid Polym. Sci*. **293**, 2249 (2015).

[28]E. Guth, *J. Appl. Phys*. **16**, 20 (1945).

[29]S. Kawahara, Y. Yamamoto, S. Fujii, Y. Isono, K. Niihara, H. Jinnai, H. Nishioka, and A. Takaoka, *Macromolocules* **41**, 4510 (2008).

[30]M. Takayanagi, H. Harima, and Y. Iwata, *J. Soc. Mater. Sci. Jpn*. **12**, 389 (1963).

[31]M. Takayanagi, S. Uemura, and S. Minami, *J. Polym. Sci., Part C: Polym. Symp*. **5**, 113 (1964).

[*Received July 2020, Revised April 2021*]